Modelling of Deep Transcranial Magnetic Stimulation: Different Coil Configurations

V. Guadagnin, M. Parazzini, I. Liorni, S. Fiocchi, and P. Ravazzani

Abstract—**This paper provides a characterization of the induced electric field distributions in the brain of a realistic human model due to 16 different coil configurations. We used the scalar potential finite element method to calculate the induced electric field distributions differentiating the brain structures, e.g. cortex, white matter, cerebellum, thalamus, hypothalamus, hippocampus, pons and midbrain. We found that, despite the presence of a depth-focality tradeoff, some configurations are able to reach subcortical white matter tracts at effective electric field level.**

I. Introduction

In recent years, the advent of deep transcranial magnetic stimulation (DTMS) allows the stimulation of deep brain region through the principle of electromagnetic induction, such as to safely and non-invasively modulate the activity of cerebral targets [1]. In particular, the induced electric field (**E**) can modify cortical excitability, increasing or decreasing it, depending on the parameters of stimulation and this can be useful for diagnostic and therapeutic purposes [2]. Indeed, several clinical studies showed that DTMS could be more effective than traditional transcranial magnetic stimulation in treating a very wide range of neurological, psychiatric and medical conditions [3], e.g. major depressive disorder [4], schizophrenia [5], bipolar depression [6], post-traumatic stress disorder [7], obsessive-compulsive disorder [1] and substance addictions [8]. In the meantime, with the purpose to increase the **E** penetration depth without inducing wider **E** spread, new coils designs have been developed [9,10]. However, the knowledge of the **E** distributions and the comparison between the different configurations of coils, that are indispensable in order to evaluate the experimental results and to optimize the therapeutic treatments, are not yet comprehensive. Indeed, to this day, these distributions have been estimated or considering each coil separately and without a comparison among different coil configurations [11], or using simplified head geometric models, such as sphere [9,10]. As it was demonstrated, the **E** distribution depends on the coil position and orientation on the scalp due to the variable shape of the head surface and the symmetric distribution obtained with a spherical model is not suitable for the most clinical applications, that requires the stimulation of a single cerebral hemisphere or of a specific target [12]. Therefore, models that faithfully reproduce the characteristics and properties of brain tissues are needed. The aim of the present study consists in characterizing and comparing the induced **E** distributions due to different configurations of coils in the brain of a realistic human head model such as to investigate in detail which cerebral regions are reached by **E** values.

V. Guadagnin, M. Parazzini, S.Fiocchi and P. Ravazzani are with the CNR Consiglio Nazionale delle Ricerche – Istituto di Elettronica e di Ingegneria dell'Informazione e delle Telecomunicazioni IEIIT, Milano 20133 Italy (corresponding author to provide phone: +39-0223993345; fax: +39-0223993367; e-mail: vanessa.guadagnin@polimi.it, marta.parazzini@polimi.it, serena.fiocchi@polimi.it, and paolo.ravazzani@polimi.it).

I. Liorni is with Dipartimento Elettronica, Informazione e Bioingegneria DEIB, Politecnico di Milano, Milano 20133 Italy, and also with CNR Consiglio Nazionale delle Ricerche – Istituto di Elettronica e di Ingegneria dell'Informazione e delle Telecomunicazioni IEIIT, Milano 20133 Italy (e-mail: ilaria.liorni@polimi.it).

II. Materials and Methods

A. Human model

The coils were placed on the head of the realistic anatomical model "Ella", a 26-years old female, of the Virtual Family [13], based on the high resolution magnetic resonance images of a healthy volunteer. In this model it is possible to clearly indentify and distinguish gray and white matter, cerebellum, thalamus, hypothalamus, hippocampus, pons and midbrain. The model was discretized with a grid resolution of 1 mm and the computational domain was limited to the upper region of the body. The dielectric properties of each tissue were assigned based on the literature data at low frequency [14,15].

B. Coil configurations

In the present study 16 different coil configurations were modelled and divided into four groups based on common geometric characteristics, as it is shown in Fig. 1. The two first designs represent the reference coils and are constituted by the circular coil and the figure-8 coil. The other 14 were selected since they are identified as the most effective for DTMS [9,10]. To the first group belong the coils characterized by two pairs of figure-8 coil arranged according to different orientations on the scalp, to the second group belong the large diameter circular coils, to the third the double cone coils, formed by two large adjacent circular windings fixed at different angles on the scalp, and to the fourth group belong the H coils, consisting of complex three-dimensional windings pattern [11,16,17]. All the coils were designed to conform to the human head model.

978-1-4244-7929-0/14/$26.00 ©2014 IEEE

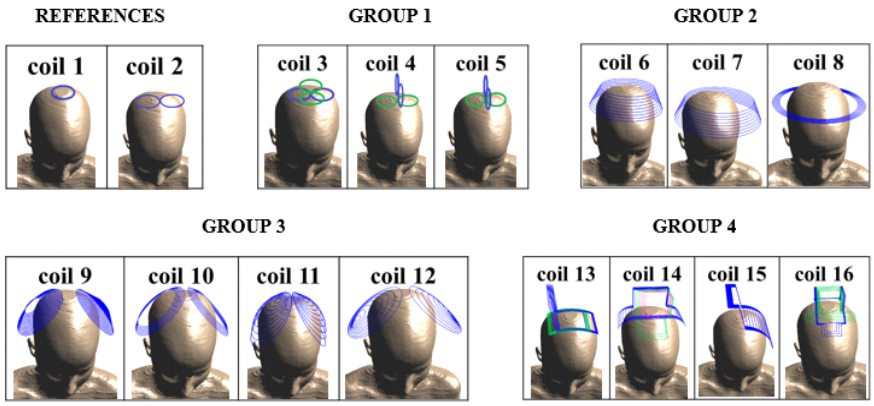

Figure 1. 16 different coil configurations modelled divided into groups based on common geometric characteristics and placed on the head of the anatomical model "Ella".

C. *Electric field simulation*

Simulations were conducted using the magneto quasi-static low-frequency solver of the simulation platform SEMCAD X (by SPEAG, www.speag.com) [18] which implements the Biot-Savart's law and is based on the scalar potential finite elements method. With the purpose to compare the different coils configurations, in all the simulations a pulse current with amplitude of 1 A and a frequency of 5 kHz was used.

D. *Electric field characterization*

For assessment of the induced **E** characteristics, for each coil, the **E** distributions were computed and analyzed in different brain structures, i.e. the cortex, the white matter, the cerebellum, the pons, the midbrain, the thalamus, the hypothalamus and the hippocampus. In particular, for each brain tissues, we estimated the percentage of volume that had **E** values equal to or greater than 10%-90% of the 99th percentile of the **E** distribution in the cortex.

In order to investigate and compare the penetration depth of each different coil configuration, we also studied the trend of **E** as a function of distance from the cortical surface comparing **E** values, normalized to the 99th percentile of the cortical **E**, at different depth from the cortex (1 cm, 2 cm, 3 cm and 4 cm) both on frontal slices common to all the coils and on the frontal slices in which each coil reaches its maximum penetration depth. Moreover, we estimated the average distance from the cortical surface of the 50% of the 99th percentile of the **E** in the cortex of each coil on the frontal and on the sagittal planes.

III. RESULTS

A. *Electric field distribution*

Fig. 2 illustrates color intensity maps of the **E** distributions in the brain induced by the two reference coils and by one configuration for each group of DTMS coils. In each panel the values are normalized with respect to the 99th percentile of the **E** distribution estimated on the cortex evaluated for each coil. It is clearly shown that varying the coil configurations induces variations in the **E** distributions in all the brain structures. Firstly, as expected, the two reference coils and the coils belonging to the first group induce the maximum electric field at the point where the windings are in contact and their **E** is localized in a small area placed on the surface regions. Indeed, the deep brain tissues are reached by very low **E** values and the **E** distribution is uniform in these structures. On the other hand, the coils belonging to the second and to the third group are able to reach deep brain structures (hippocampus, pons, midbrain, thalamus and hypothalamus), with **E** values ranging between the 20-30% of the maximum in the cortex but, at the same time, they induce in almost all the cortical surface **E** values higher than 50% of the maximum. Finally, the H coils, belonging to the fourth group, reduce the **E** spread on the surface regions with respect to the second and to the third group but are not able to reach the same **E** values as these groups in deep brain structures.

B. *Coil penetration depth*

In Fig. 3 is shown the trend of **E** as a function of distance from the cortical surface for each coil configurations. The **E** values are normalized respect to the 99th percentile of the **E** distribution in the cortex, evaluated for each coil configuration. It can be seen that the rate of decay of **E** with distance is significantly quicker for the reference coils, especially for the circular coil, and for the coils of the first group compared to the other configurations. In fact, the **E** values of these first coils at a depth of 4 cm are equal to 30-40% of the maximum and to 20% of the maximum for the circular coil. The coils belonging to the second and to the

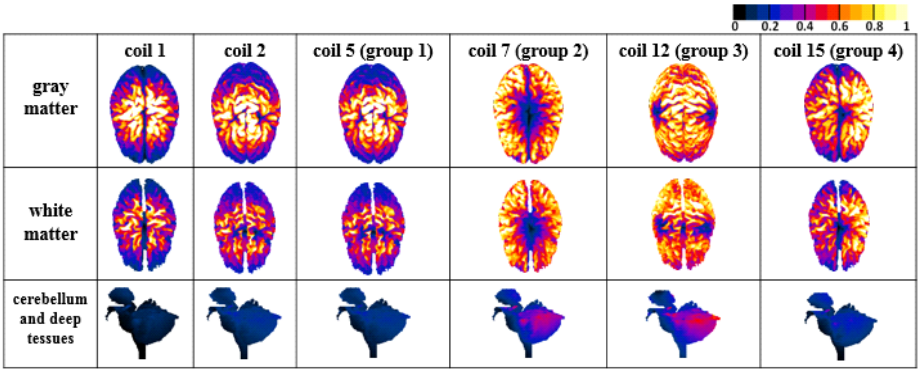

Figure 2. Surface distributions of the induced **E** in the cortex (1st row), white matter (2nd row) and cerebellum with deep brain tissues (3rd row) for the reference coils and for one coil of each group. The field amplitudes are normalized respect to the 99th percentile of the **E** distribution in the cortex.

third group attenuate the degree of reduction of the induced **E** with the increase of distance: the **E** values at a depth of 4 cm are respectively equal on average to 55% and to 60% of the maximum. At last, the **E** decay profile as a function of distance from the cortical surface of the H coils is more slower than the references and than the first group, but faster than the second and than the third group of coils. Indeed, the **E** values at a depth of 4 cm ranging between 47% and 55% of the maximum.

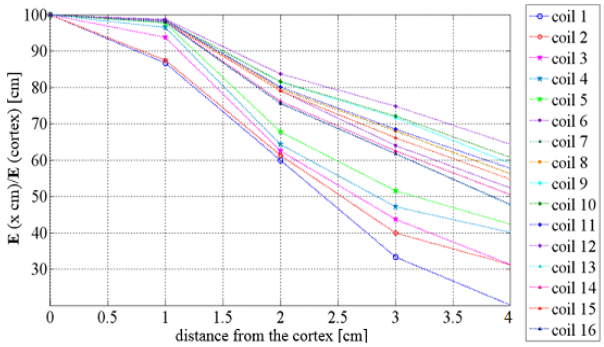

Figure 3. **E** values, normalized respect to the 99th percentile of the **E** distribution in the cortex, at increasing distance from the cortical surface, for the 16 coil configurations on the frontal slices in which each coil reaches its maximum penetration depth.

In the case of the single circular coil, the average distance from the cortical surface of the 50% of the 99th percentile of the **E** evaluated in the cortex on different frontal and sagittal planes is approximately equal to 2 cm. For the figure-8 coil and for the coils belonging to the first group it is below 3 cm. The coils of the second group, on the other hand, increase the average depth of the 50% of the 99th percentile of the **E** in the cortex, up to 3.5 cm. The coils belonging to the third group are characterized by the highest depth values, ranging between 3.5 cm and 4.5 cm, on both planes. Finally, for the coils of the fourth group the average depth on both the planes ranges between 3 cm and 3.5 cm.

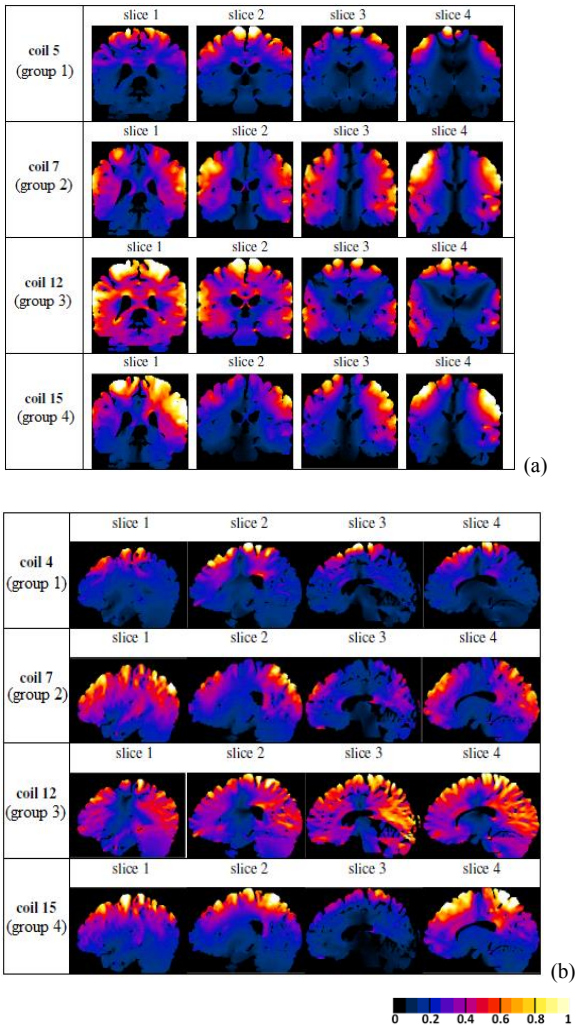

Figure 4. Frontal (a) and sagittal (b) slices of the coil of each group that reaches the highest penetration depth from the cortical surface of the 50% of the 99th percentile of the **E** in the cortex. The mean between **E** penetration depth values of these slices returns the average distance of the 50% of the 99th percentile of the **E** in the cortex on the frontal and on the sagittal planes. The field amplitudes are normalized respect to the 99th percentile of the **E** distribution in the cortex.

IV. Conclusion

The quantification of the induced **E** distributions adopting a consistent set of metrics and using a realistic human head model achieved in this study has allowed to obtain objective and accurate results, differentiated for each brain structure. The results shows that, for each coil design, the ability to directly stimulate deeper brain structures is obtained at the expense of inducing wider **E** spread on the cortical surface. Interestingly, some configurations (particularly the coils belonging to the second and to the third group and the H coils) result to be able to reach effective stimulation of subcortical white matter tracts. On the contrary, few coils are able to reach deeper brain structures with **E** values greater than 20% of the maximum. In conclusion, this study shows how the characterization of the **E** distributions could play an important role in the optimization of the geometry and of the position on the scalp of the coils and can help clinicians in the choice of the coil more suitable to fulfill the needs of a specific treatment.

Acknowledgment

The authors wish to thank Schmid & Partner Engineering AG (www.speag.com) for having provided the simulation software SEMCAD X.

References

[1] Y. Roth, F. Padberg, A. Zangen, "Transcranial magnetic stimulation of deep brain region: principles and methods", Adv. Biol. Psychiatry, vol. 23, pp. 204-224, 2007.
[2] T. Wagner, A. Valero-Cabre, A. Pascual-Leone, "Non-invasive human brain stimulation", Annu. Rev. Biomed. Eng., vol. 9, pp. 527-565, 2007.
[3] F. S. Bersani, A. Minichino, P. G. Enticott, L. Mazzarini, N. Khan et al., "Deep transcranial magnetic stimulation as a treatment for psychiatric disorders: a comprehensive review", Eur. Psychiatry, vol. 28(1), pp. 30-39, 2013.
[4] Y. Levkovitz, E. V. Harel, Y. Roth, Y. Braw, D. Most et al., "Deep transcranial magnetic stimulation over the prefrontal cortex: evaluation of antidepressant and cognitive effects in depressive patients", Brain Stimul., vol. 2(4), pp. 188-200, 2009.
[5] Y. Levkovitz, L. Rabany, E. V. Harel, A. Zangen, "Deep transcranial magnetic stimulation add-on for treatment of negative symptoms and cognitive deficits of schizophrenia: a feasibility study", Int. J. Neuropsychopharmacol., vol. 14(7), pp. 991-996, 2011.
[6] E. V. Harel, A. Zangen, Y. Roth, I. Reti, Y. Braw et al., "H-coil repetitive transcranial magnetic stimulation for the treatment of bipolar depression: an add-on, safety and feasibility study", World J. Biol. Psychiatry, vol. 12, pp. 119-126, 2011.
[7] M. Isserles, A. Y. Shalev, Y. Roth, T. Peri, I. Kutz et al., "Effectiveness of deep transcranial magnetic stimulation combined with a brief exposure procedure in post-traumatic stress disorder – a pilot study", Brain Stimul., vol. 6, pp. 377-383, 2013.
[8] C. Rapinesi, G. D. Kotzalidis, D. Serata, A. Del Casale, F. S. Bersani et al., "Efficacy of add-on deep transcranial magnetic stimulation in comorbid alcohol dependence and dysthymic disorder: three case reports", Prim. Care Companion CNS Disord., vol. 15(1), 2013.
[9] Z. D. Deng, S. H. Lisanby, A. V. Peterchev, "Electric field depth-focality tradeoff in transcranial magnetic stimulation: simulation comparison of 50 coil design", Brain Stimul., vol. 6, pp. 1-13, 2013.
[10] Z. D. Deng, S. H. Lisanby, A. V. Peterchev, "Coil design considerations for deep transcranial magnetic stimulation", Clin. Neurophysiol., vol. 125, pp. 1202-1212, 2014.
[11] Y. Roth, A. Amir, Y. Levkovitz, A. Zangen, "Three-dimensional distribution of the electric field induced in the brain by transcranial magnetic stimulation using figure 8 and deep H-coils", J. Clin. Neurophysiol., vol. 24, pp. 31-38, 2007.
[12] Y. Roth, G. S. Pell, A. Zangen, "Commentary on: Deng et al., Electric field depth-focality tradeoff in transcranial magnetic stimulation: simulation comparison of 50 coil designs", Brain Stimul., vol. 6, pp. 14-5, 2013.
[13] A. Christ, W. Kainz, E. G. Hahn, K. Honegger, M. Zefferer et al., "The virtual family- development of surface-based anatomical models of two adults and two children for dosimetric simulations", Phys Med. Biol., vol. 55, pp. N23-N38, 2010.
[14] S. Gabriel, R. W. Lau, C. Gabriel, "The dielectric properties of biological tissues: II. Measurements in the frequency range of 10 Hz to 20 GHz", Phys Med. Biol., vol. 41, pp. 2251-2269, 1996b.
[15] C. Gabriel, A. Peyman, E. H. Grant, "Electrical conductivity of tissue at frequencies below 1 MHz", Phys Med. Biol., vol. 54, pp. 4863-4878, 2009.
[16] A. Zangen, Y. Roth, B. Voller, M. Hallet, "Transcranial magnetic stimulation of deep brain regions: evidence for efficacy of the H-coil", Clin. Neurophysiol., vol. 116, pp. 775-779, 2005.
[17] A. Zangen, Y. Roth, P. C. Miranda, D. Hazani, M. Hallet, "Transcranial magnetic stimulation, systems and methods", U.S. Patent 0288365, November 24, 2011.
[18] SEMCAD X v14.8 by SPEAG, Available at www.speag.com.